PRACE INSTYTUTU ODLEWNICTWA
Tom LI Rok 2011 Zeszyt 4

DOI: 10.7356/iod.2011.13

STUDIES OF THEORETICAL AND PRACTICAL ASPECTS OF THE DESIGN OF MATERIALS LIGHTER THAN AIR

PRACE STUDIALNE NAD TEORETYCZNYMI I PRAKTYCZNYMI ASPEKTAMI PROJEKTOWANIA MATERIAŁÓW LŻEJSZYCH OD POWIETRZA

Jerzy J. Sobczak[1], Ludmil B. Drenchev[2]

[1]Foundry Research Institute, 73 Zakopianska Street, 30-418 Krakow, Poland
[2]Institute of Metal Science, 67 Shipchenski Prohod Street, 1574 Sofia, Bulgaria

Abstract

This paper discusses some theoretical aspects of the design of ultralight materials. Potential application of syntactic foams in the fabrication of composites lighter than air is also analyzed. Carbon allotropic forms (fullerenes, colossal carbon tubes) and some non-carbon matters are considered as components of ultralight composites. Calculations for the size of fullerenes, the number of carbon atoms in their structure and thickness of reinforcing phase are presented. It is concluded that 3D carbon molecules (fullerenes) and colossal carbon tubes are the most promising components for design of ultralight metallic materials which can be lighter than air.

Key words: ultralight materials, composites, syntactic foams, carbon allotropic forms

Streszczenie

W artykule omówiono wybrane teoretyczne aspekty projektowania ultralekkich materiałów kompozytowych. Przeanalizowano potencjalne zastosowanie pian syntektycznych w produkcji kompozytów lżejszych od powietrza. Uwzględniono alotropowe odmiany węgla (fulereny, „kolosalne" nanorurki węglowe), jak również niektóre substancje niewęglowe mogące znaleźć zastosowanie jako komponenty ultralekkich kompozytów. Podano wzory, które pozwalają obliczyć wielkość fulerenów, liczbę atomów węgla w ich strukturze i grubość ścianek fazy zbrojącej. Stwierdzono, że cząsteczki węgla 3D (fulereny) i nanorurki węgla o makrorozmiarach stanowią najbardziej obiecujące substancje do projektowania ultralekkich materiałów o gęstości mniejszej od gęstości powietrza.

Słowa kluczowe: ultralekkie materiały, kompozyty, piany syntaktyczne, alotropowe odmiany węgla

Introduction

There is no doubt that ultralight materials will play an increasingly important role in construction of different machines and specific components not only in automotive and space industry but also in all other industrial branches. This paper is devoted to some basic principles for the design of ultralight metallic materials, and especially for the design of metallic materials lighter than air. The aim of this paper is to analyze the geometrical and physical parameters of the components of ultralight materials and to discuss various geometrical parameters–weight combinations for some virtual metallic materials lighter than air.

Reasonably, the object of consideration here will be metallic materials with closed porosity. There are various groups of such materials: gasars [1], conventional foams, syntactic foams [2], partially infiltrated open porosity preforms. All these materials can be considered as a specific class of metal matrix composites. The effective density of the materials (gasars and conventional foams), ρ_S (kg·m^{-3}), can be expressed by relation

$$\rho_s = \frac{V_g\rho_g + V_m\rho_m}{V_g + V_m} \tag{1}$$

where V_g, V_m, ρ_g and ρ_m are total volume of pores, volume of metal matrix, gas density and metal matrix density, respectively. Taking into account that porosity, ε, is defined by relation

$$\varepsilon = \frac{V_g}{V_g + V_m} \tag{2}$$

Formula (1) can be written as

$$\rho_s = \varepsilon\rho_g + (1-\varepsilon)\rho_m \tag{3}$$

which gives correlation between material porosity and the densities

$$\varepsilon = \frac{\rho_m - \rho_s}{\rho_m - \rho_g} \tag{4}$$

This formula allows calculating of the porosity level, which should be reached if one wants to obtain material with certain density ρ_S is to be obtained. For example, if a porous material made from aluminum (ρ_m = 2700 kg·m^{-3}) as matrix and pores full of helium (ρ_g = 0.1785 kg·m^{-3}), see Table 1, should be of density ρ_S = 1.2 kg·m^{-3}, the porosity of the material must be ε = 0.99962. If a porous material is made from Mg-Ni alloy (ρ_m = 1000 kg·m^{-3}) as matrix and pores are filled again with helium, the porosity of the material must be ε = 0.99898. Let us mention that this porosity relates to materials with density equal to that of air.

Table 1. Density of some materials used in calculations under normal conditions [3]

Tabela 1. Gęstość w warunkach normalnych niektórych materiałów stosowanych w obliczeniach [3]

Material	ρ_m, **kg·m^{-3}**	**Material**	ρ_g, **kg·m^{-3}** (24°C, 0.1 MPa)
Al	2700	air	1.2
Mg	1740	He	0.1785
Li	531	Ar	1.784
Al_2O_3	3200	H_2	0.0899
Mg-Li alloy	1000	N	1.251

I. Porosity and density of some conventional porous materials

The form of pores in a porous material is different but usually there is a geometrical shape that dominates. For example, typical gasar pores are near cylindrical, Fig. 1 a), and pores in conventional foams are near spherical, Fig. 1 b). The peculiarity of these two materials is that their porosity is in-situ obtained. Metallic syntactic foams are in-vitro obtained porous materials and their pores are strongly spherical. For example, syntactic foam can be obtained from fly ash (glassy-like cenospheres) and metallic matrix, Fig. 1 c) and d) [2].

Ordered porosity materials (gasars)

In the case of gasars, for the purpose of simplicity, the pores can be considered identical and strongly cylindrical with radius r_1, ordered in a periodic structure represented by a set of regular polygonal cells [4]. A circle of equivalent area and radius r_2 replaces the polygonal cell of the periodic structure, Fig. 2 a), and formally the structure can be considered as composed from aligned cylindrical tubes with wall thickness $\Delta r = r_2 - r_1$. The porosity of such structure can be obtained approximately by expression

$$\varepsilon = \frac{r_1^2}{r_2^2} \tag{5}$$

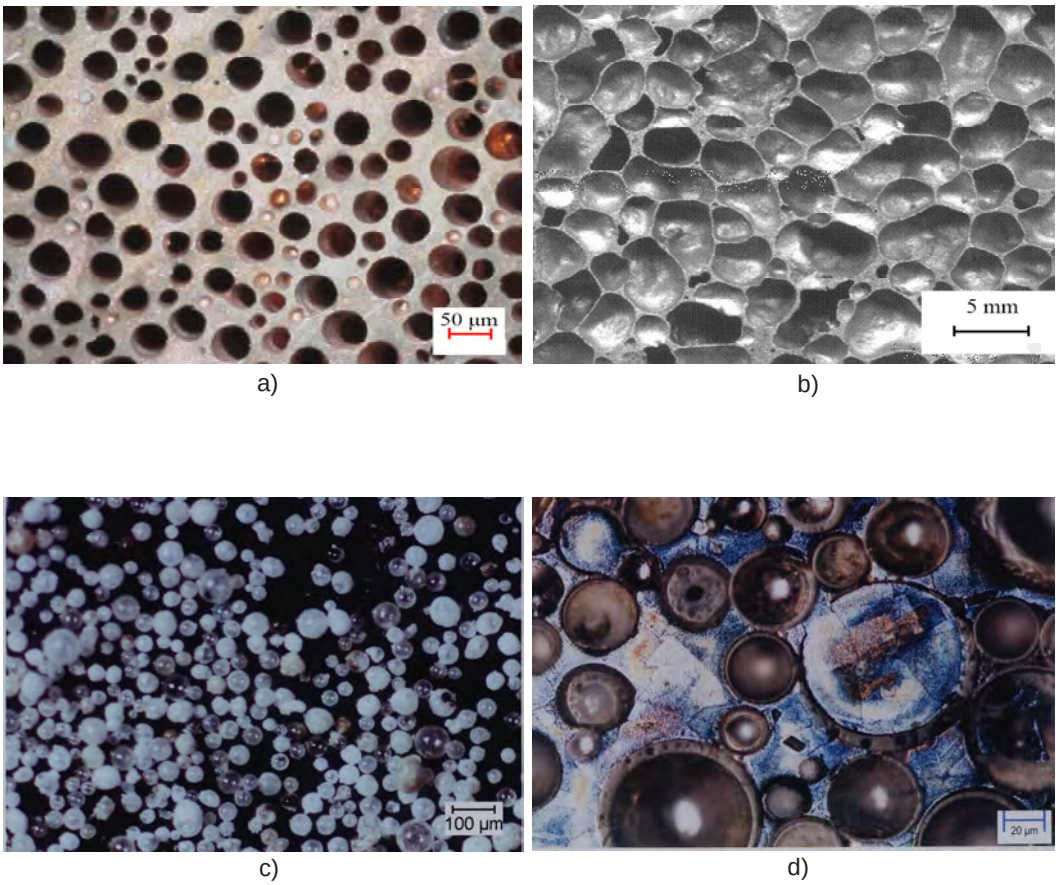

Fig. 1. View of various porous materials: a) cross-section of copper gasar [5]; b) cross-section of aluminum foam [6]; c) as-received fly ash, glassy-like cenospheres [7]; d) structure of Pb/60 vol.% fly ash syntactic foam [7]

Rys. 1. Widok struktury różnych materiałów porowatych: a) przekrój poprzeczny gazaru miedziowego [5]; b) przekrój poprzeczny piany aluminiowej [6]; c) szkliste cenosfery popiołu lotnego bezpośrednio po otrzymaniu [7]; d) struktura piany syntaktycznej Pb/60% obj. popiołu lotnego [7]

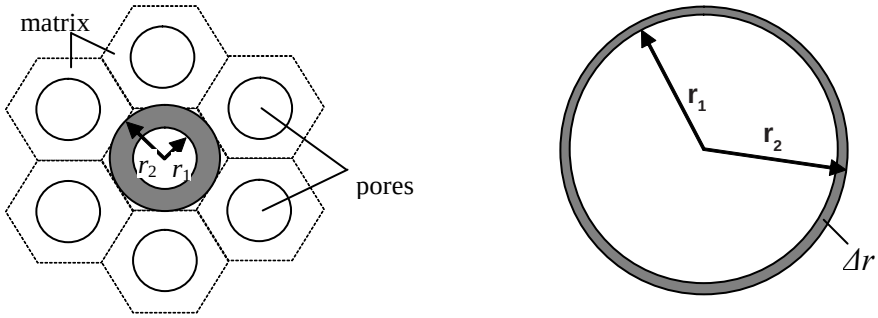

Fig. 2. Schemes for porosity calculation: a) geometrical model of uniform cylindrical pore distribution in gasars; b) representation of single spherical bubble with wall thickness Δr

Rys. 2. Schemat do obliczania porowatości: a) geometryczny model równomiernego rozkładu cylindrycznych porów w gazarach; b) schematyczne przedstawienie pojedynczej banieczki o grubości ścianki Δr

If we fix the porosity ε and the radius r_2, the radius r_1 can be obtained by (5) and then the wall thickness Δr can be calculated. The results for Al and Mg-Li gasars with density ρ_S equal to the air density are given in Table 2.

Table 2. Pore size and pore wall thickness for some metallic gasars. Material density ρ_S = 1.2 kg·m^{-3}

Tabela 2. Wielkość porów i grubość ścianek porów w niektórych gazarach metalicznych. Gęstość materiału ρ_S = 1,2 kg·m^{-3}

Matrix	**Al** (ε = 0.99962)			**Mg-Li alloy** (ε = 0.99898)		
r_2, **m**	1 x 10^{-3}	100 x 10^{-6}	10 x 10^{-6}	1 x 10^{-3}	100 x 10^{-6}	10 x 10^{-6}
Δr, **m**	0.19 x 10^{-6}	19 x 10^{-9}	1.9 x 10^{-9}	0.51 x 10^{-6}	51 x 10^{-9}	5.1 x 10^{-9}

Gasar technology is based on preliminary gas saturation of a melt which solidified under unidirectional cooling. The melt saturation takes place under elevated gas (usually hydrogen) pressure according to Sievert's law [1], while solidification runs under lower pressure. Theoretically, such high final porosity can be reached after gas saturation under extremely high pressure, which changes essentially the phase diagram of the system. Moreover, crucial reduction of the pressure during solidification will cause quasi boiling process and great quantity of gas will leave the melt. The latter effect will result in reduction of final porosity. There are additional essential reasons to conclude that the gasar technology cannot be applied for production of extremely high porous materials. Up to now, the production of gasars of maximum porosity of about 0.75 has been reported which is very far from what is required for a material lighter than air.

Conventional foams

The same assumptions can be made for conventional foams and the porosity can be obtained approximately by expression

$$\varepsilon = \frac{r_1^3}{r_2^3} \tag{6}$$

The pore wall thickness values calculated by this formula for Al and Mg-Li conventional foams are given in Table 3.

Table 3. Pore size and pore wall thickness for two metallic foams. Material density ρ_S = 1.2 kg·m^{-3}

Tabela 3. Wielkość porów i grubość ścianek porów w dwóch pianach metalicznych. Gęstość materiału ρ_S = 1,2 kg·m^{-3}

Matrix	**Al** (ε = 0.99962)			**Mg-Li alloy** (ε = 0.99898)		
r_2, **m**	1 x 10^{-3}	100 x 10^{-6}	10 x 10^{-6}	1 x 10^{-3}	100 x 10^{-6}	10 x 10^{-6}
Δr, **m**	0.13 x 10^{-6}	13 x 10^{-9}	1.3 x 10^{-9}	0.34 x 10^{-6}	34 x 10^{-9}	3.4 x 10^{-9}

It seems that, compared with gasars, conventional foams are more suitable for the fabrication of ultralight materials. One principal disadvantage of the conventional foams is relatively small achievable bubble wall thickness. This can be seen in Table 3. For aluminum foam with porosity ε = 0.99962, if the bubbles are of a 1 mm radius, the bubble wall thickness is 0.13 nm. Solid aluminum possesses a face centered cubic (fcc) cell with the size of about 0.405 nm, which means that the bubble wall will consist of about 320 elementary layers. It is not sure that such a wall thickness can be produced by the foaming process and that this will be enough to provide for mechanical strength of the foam obtained. For bubble size of less than 1 mm, the wall thickness becomes

extremely small (see Table 3) and difficult or even impossible to be reached by foaming of any melt. Other problems arise with foaming agents, gas used and particular values of the surface tension (because of capillarity phenomena) specific for metal/gas system under consideration. All these parameters and relations between them need to be investigated theoretically and experimentally before the commencement of technology elaboration.

Metallic syntactic foams

Syntactic foams give better opportunity for design of ultralight metallic materials. These foams consist of ceramic or metallic cenospheres homogeneously distributed in metal matrix. Their advantage is that the cenospheres (bubbles) could be preliminarily obtained by means of various technologies and materials. For example, fly ash (Fig. 1c)), which is a component of waste product of coal power stations, consists of empty spheres of different oxides. Such spheres can also be produced from alumina, Mg-Li alloy, carbon or other substances. In this case, the most essential problem is how to pack and to stick the bubbles to form an integrated body. Modern materials and technologies offer a great variety of possibilities that must be tested carefully.

Let us consider that a variety of cenospheres made from different substances is available. Here we will discuss porous materials, which consist of close packed cenospheres, infiltrated or not infiltrated by liquid metal. Let us consider two configurations of spheres as shown in Fig. 3 a) and b).

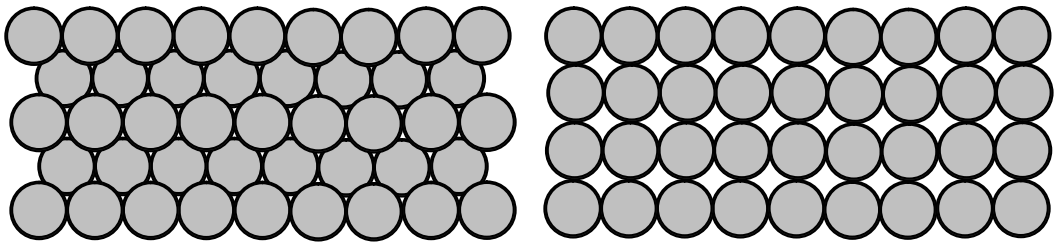

Fig. 3. Configurations of close packed cenospheres containing open pores: a) an arrangement with minimum open porosity equal to 0.258; b) an arrangement with maximum open porosity equal to 0.476

Rys. 3. Konfiguracje cenosfer o bliskim upakowaniu zawierające otwarte pory: a) układ o najmniejszej otwartej porowatości wynoszącej 0,258; b) układ o największej otwartej porowatości wynoszącej 0,476

The configurations similar to those in Figure 3 have three components:

1. The total volume, V_m, of the space between the bubbles constituting the open porosity of the material;
2. the volume, V_g, of the space in all the bubbles constituting the closed porosity of the material; and
3. the total volume, V_b, of the space occupied by material from which the bubbles are made, i. e. by the bubble walls.

The total volume of the porous body is $V_S = V_m + V_g + V_b$. The elementary cells corresponding to these configurations are shown in Fig. 4. It is easy to be shown that the

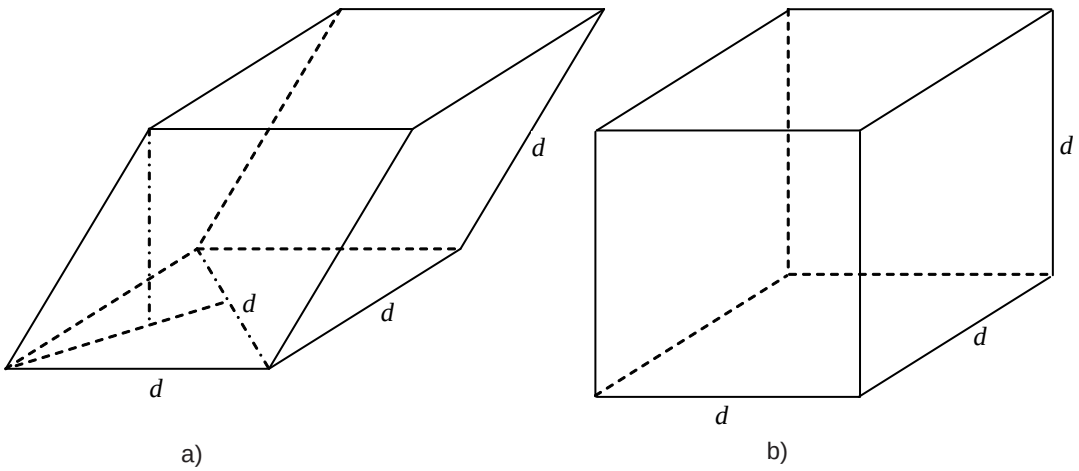

Fig. 4. Elementary cells of closely packed spheres: a) rhomboidal, related to configuration in Fig. 3 a); b) cubic, related to configuration in Fig. 3 b)

Rys. 4. Elementarne komórki ściśle upakowanych elementów kulistych: a) romboidalne związane z konfiguracją przedstawioną na rysunku 3 a); b) sześcienne związane z konfiguracją na rysunku 3 b)

configuration in Fig. 3 a) is of minimum open porosity and the configuration in Fig. 3 b) is of maximum open porosity, which can be reached by close packed spheres. An important fact is that the open porosity in the above two configurations does not depend on bubble size. Its minimum value $\varepsilon_{min} = 0.258$ is related with an arrangement in Fig. 3 a) and the maximum value $\varepsilon_{max} = 0.476$ is related with an arrangement in Fig. 3 b). Each arbitrary arrangement of bubbles in a porous material will possess open porosity ε between these values, $\varepsilon_{min} < \varepsilon < \varepsilon_{max}$. The porous materials considered can be characterized by a set complex of three dimensionless numbers, (M_m, M_g, M_b). These numbers represent the individual contribution of the above listed components to the material density. The number M_m is the relative fraction of the density, which corresponds to the substance in open porosity (the contribution of the open porosity), M_g is the relative fraction of the density, which corresponds to the content (fluid or vacuum) of the bubbles (the contribution of the closed porosity) and the number M_b is the relative fraction of the density, which corresponds to the bubble wall substance (the contribution of the bubble walls). Following this description for a material of volume V_S, the following can be written

$$M_m = \frac{\rho_m V_m / V_s}{(\rho_m V_m + \rho_g V_g + \rho_g V_g) V_s} \tag{7}$$

$$M_g = \frac{\rho_g V_g / V_s}{(\rho_m V_m + \rho_g V_g + \rho_g V_g) V_s} \tag{8}$$

$$M_g = \frac{\rho_b V_b / V_s}{(\rho_m V_m + \rho_g V_g + \rho_b V_b) V_s} \tag{9}$$

Obviously $M_m + M_g + M_b = 1$. The set of these three numbers is very useful because it gives information on what is the most effective way to decrease or to increase the material density. The number of the highest value indicates the major component, which contributes to the density of the material. For example, if M_m has the highest value in the whole set related with a certain material, it means that the substance in open porosity has the highest contribution to the material density. If one wants to reduce the material density, the most effective way will be to reduce the density of this substance but without changing the parameters of other two components. This will be demonstrated in the examples below.

Various combinations of cenosphere parameters, bubble materials and obtained material density are given in Table 4. The calculations are made for an arrangement with rhomboidal cells, see Fig. 4 a). To change such combination of cenospheres into an integrated body, the cenospheres must be “stuck” and/or covered with thin coating. If the cenospheres are preliminarily “glued”, the obtained porous body can be infiltrated with liquid metal to form a monolithic material. Another option is to evacuate all gases from the porous body of open porosity and after this to coat only the surface of the body with metal melt. After the metal solidification, this body will be an integrated non-permeable material. The results obtained for both variants can be found in Table 4. An increase of density due to material coating is not included in the results. If the thickness of such coating is 0.1 x 10^{-3} m and the density of the coating material is 1000 kg·m^{-3} (Mg-Li alloy), the density of the material will increase by about 0.5 kg·m^{-3}.

Table 4. Parameters of porous materials made from cenospheres, an arrangement with rhomboidal cell

Tabela 4. Parametry porowatych materiałów wytwarzanych z cenosfer, układ z komórkami romboidalnymi

No.	r_2, m	Δr, m	Bubble material	Gas in bubble	Material in open porosity	Density of material, kg·m^{-3}	(M_m, M_g, M_b)
1	0.4 x 10^{-3}	2.0 x 10^{-6}	Al_2O_3	air	Al	1021.0	(0.964, 0.001, 0.035)
2	0.4 x 10^{-3}	2.0 x 10^{-6}	Al_2O_3	air	Mg-Li	401.2	(0.909, 0.002, 0.089)
3	0.4 x 10^{-3}	2.0 x 10^{-6}	Al_2O_3	air	Vacuum	36.32	(0.000, 0.026, 0.974)
4	0.4 x 10^{-3}	2.0 x 10^{-6}	Al_2O_3	He	Vacuum	35.51	(0.000, 0.004, 0.996)
5	0.4 x 10^{-3}	2.0 x 10^{-6}	Al_2O_3	H_2	Vacuum	35.44	(0.000, 0.002, 0.998)
6	0.4 x 10^{-3}	2.0 x 10^{-6}	Al	air	Vacuum	30.79	(0.000, 0.031, 0.969)
7	0.4 x 10^{-3}	2.0 x 10^{-6}	Mg-Li	air	Vacuum	12.00	(0.000, 0.078, 0.922)
8	0.2 x 10^{-3}	0.2 x 10^{-6}	Mg-Li	air	Vacuum	3.173	(0.000, 0.300, 0.700)
9	0.4 x 10^{-3}	0.2 x 10^{-6}	Mg-Li	air	Vacuum	2.065	(0.000, 0.462, 0.538)
10	0.5 x 10^{-3}	0.2 x 10^{-6}	Mg-Li	air	Vacuum	1.843	(0.000, 0.518, 0.482)
11	50 x 10^{-6}	10 x 10^{-9}	Al_2O_3	He	Vacuum	1.554	(0.000, 0.085, 0.915)
12	0.5 x 10^{-3}	0.1 x 10^{-6}	Al_2O_3	H_2	Vacuum	1.489	(0.000, 0.045, 0.955)
13	0.5 x 10^{-3}	0.1x10^{-6}	Mg-Li	air	Vacuum	1.399	(0.000, 0.682, 0.318)
14	0.3 x 10^{-3}	50 x 10^{-9}	Al	He	Vacuum	1.132	(0.000, 0.117, 0.883)
15	0.7 x 10^{-3}	0.1 x 10^{-6}	Al_2O_3	H_2	Vacuum	1.082	(0.000, 0.061, 0.939)
16	0.3 x 10^{-3}	50 x 10^{-9}	Al	H_2	Vacuum	1.066	(0.000, 0.062, 0.938)
17	0.5 x 10^{-3}	200 x 10^{-9}	Mg-Li	H_2	Vacuum	0.955	(0.000, 0.070, 0.930)
18	0.5 x 10^{-3}	50 x 10^{-9}	Al_2O_3	He	Vacuum	0.843	(0.000, 0.157, 0.843)
19	0.5 x 10^{-3}	0.1 x 10^{-6}	Mg-Li	He	Vacuum	0.577	(0.000, 0.229, 0.771)
20	0.7 x 10^{-3}	50 x 10^{-9}	Al_2O_3	H_2	Vacuum	0.575	(0.000, 0.116, 0.884)
21	0.7 x 10^{-3}	0.1 x 10^{-6}	Mg-Li	H_2	Vacuum	0.384	(0.000, 0.173, 0.827)
22	0.5 x 10^{-3}	10 x 10^{-9}	Al_2O_3	He	Vacuum	0.275	(0.000, 0.481, 0.519)

All combinations after the 13th item in the table above are of density lower than the air density. The combinations after the 18th item give density lower than the air density even after the application of Mg-Ni alloy coating of 0.1 x 10^{-3} m thickness.

The same calculations are repeated for an arrangement with cubic cells. The results are given in Table 5. Here, because of greater percentage of open porosity, all combinations after the 10th item guarantee material density lower than the air density and the combinations after the16th item result in density lower than the air density even after the application of a coating as mentioned above.

Table 5. Parameters of porous materials made from cenospheres, arrangement with cubic cell

Tabela 5. Parametry porowatych materiałów wytwarzanych z cenosfer, układ z komórkami sześciennymi

No	r_2, m	Δr, m	Bubble material	Gas in bubble	Material in open porosity	Density of material, kg·m^{-3}	(M_m,M_g,M_b)
1	0.4 x 10^{-3}	2.0 x 10^{-6}	Al_2O_3	air	Al	1311.0	(0.980, 0.005, 0.015)
2	0.4 x 10^{-3}	2.0 x 10^{-6}	Al_2O_3	air	Mg-Li	501.7	(0.949, 0.013, 0.038)
3	0.4 x 10^{-3}	2.0 x 10^{-6}	Al_2O_3	air	Vacuum	25.68	(0.000, 0.026, 0.974)
4	0.4 x 10^{-3}	2.0 x 10^{-6}	Al_2O_3	He	Vacuum	25.11	(0.000, 0.004, 0.996)
5	0.4 x 10^{-3}	2.0 x 10^{-6}	Al_2O_3	H_2	Vacuum	25.06	(0.000, 0.002, 0.998)
6	0.4 x 10^{-3}	2.0 x 10^{-6}	Al	air	Vacuum	21.77	(0.000, 0.031, 0.969)
7	0.4 x 10^{-3}	2.0 x 10^{-6}	Mg-Li	air	Vacuum	8.483	(0.000, 0.078, 0.922)
8	0.2 x 10^{-3}	0.2 x 10^{-6}	Mg-Li	air	Vacuum	2.244	(0.000, 0.300, 0.700)
9	0.4 x 10^{-3}	0.2 x 10^{-6}	Mg-Li	air	Vacuum	1.460	(0.000, 0.462, 0.538)
10	0.5 x 10^{-3}	0.2 x 10^{-6}	Mg-Li	air	Vacuum	1.303	(0.000, 0.518, 0.482)
11	50 x 10^{-6}	10 x 10^{-9}	Al_2O_3	He	Vacuum	1.099	(0.000, 0.085, 0.915)
12	0.5 x 10^{-3}	0.1 x 10^{-6}	Al_2O_3	H_2	Vacuum	1.053	(0.000, 0.045, 0.955)
13	0.5 x 10^{-3}	0.1 x 10^{-6}	Mg-Li	air	Vacuum	0.990	(0.000, 0.682, 0.318)
14	0.3 x 10^{-3}	50 x 10^{-9}	Al	He	Vacuum	0.117	(0.000, 0.117, 0.883)
15	0.7 x 10^{-3}	0.1 x 10^{-6}	Al_2O_3	H_2	Vacuum	0.765	(0.000, 0.061, 0.939)
16	0.3 x 10^{-3}	50 x 10^{-9}	Al	H_2	Vacuum	0.754	(0.000, 0.062, 0.938)
17	0.5 x 10^{-3}	200 x 10^{-9}	Mg-Li	H_2	Vacuum	0.675	(0.000, 0.070, 0.930)
18	0.5 x 10^{-3}	50 x 10^{-9}	Al_2O_3	He	Vacuum	0.596	(0.000, 0.157, 0.843)
19	0.5 x 10^{-3}	0.1 x 10^{-6}	Mg-Li	He	Vacuum	0.408	(0.000, 0.229, 0.771)
20	0.7 x 10^{-3}	50 x 10^{-9}	Al_2O_3	H_2	Vacuum	0.406	(0.000, 0.116, 0.884)
21	0.7 x 10^{-3}	0.1 x 10^{-6}	Mg-Li	H_2	Vacuum	0.272	(0.000, 0.173, 0.827)
22	0.5 x 10^{-3}	10 x 10^{-9}	Al_2O_3	He	Vacuum	0.194	(0.000, 0.481, 0.519)

2. Carbon allotropic forms as a constitutional phase in ultralight synthetic foams

It can be said that graphene became most popular carbon atomic crystal especially after Nobel Prize for Physics in 2010. Graphene is 2D carbon molecule which is composed of linked hexagonal rings in the form of sheet. Fullerenes are specific class of large 3D carbon molecules. Their structure is very similar to graphene sheets. Because of 3D nature of a fullerene, it contains not only hexagonal rings but also pentagonal or even heptagonal rings in his construction. Fullerenes are in the shape of sphere (buckyball), ellipsoid, tube (buckytube or nanotube), or combination of the three elements [8]. The most important feature of fullerenes is their monolayer structure resembling folded graphene which gives reason to call them 3D atomic crystals, Fig. 5. An interesting structure of built-in spherical fullerenes named “bucky onion” was found by Sumio Iijima [9].

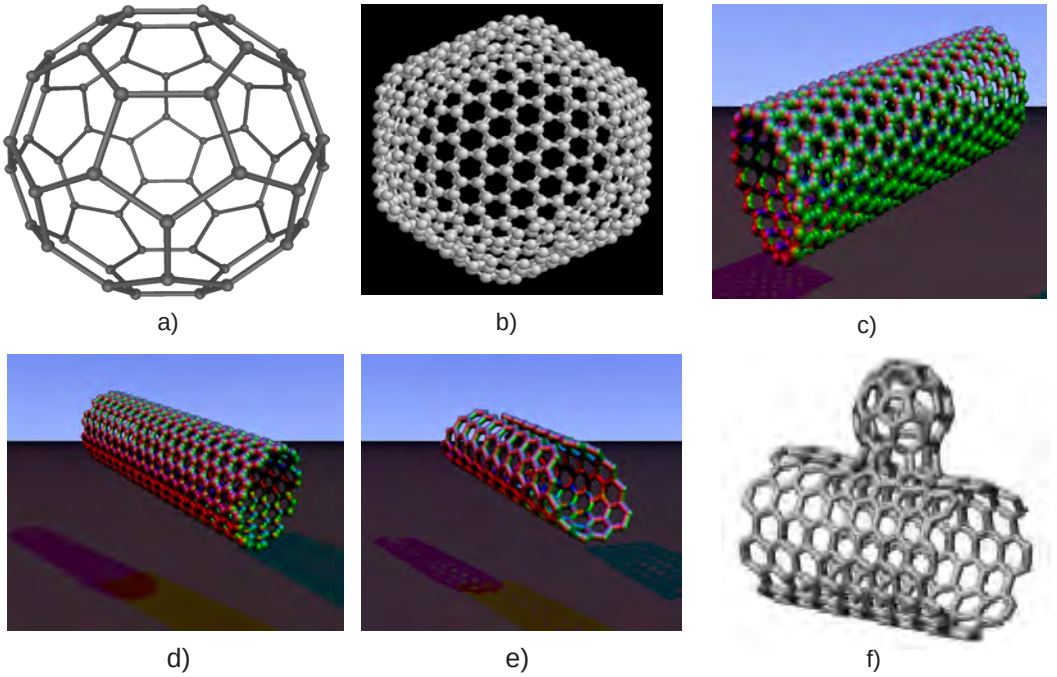

Fig. 5. Schematic representations of some fullerenes: a) C_{60}; b) C_{540}; c) zigzag nanotube; d) armchair nanotube; e) chiral nanotube; f) nanobud structure (armchair nanotube combined with buckyball) - after [10, 11]

Rys. 5. Schematyczne przedstawienie niektórych fulerenów: a) C_{60}; b) C_{540}; c) nanorurki zygzakowate; d) nanorurki fotelowe; e) nanorurki chiralne (skręcone); f) struktura nanopączków (połączenie nanorurki fotelowej z „piłeczką Bucky'ego") - wg [10, 11]

Fullerenes together with graphene, graphite, diamond, colossal carbon tubes and amorphous carbon are elements of known carbon allotropes. The two-dimensional (graphene) and the three-dimensional (fullerenes) atomic crystals are subjects of intensive research because of their extraordinary chemical and physical properties and also their potential application in material science, nanotechnology and electronics.

There are various reasons to consider fullerenes to be serious candidates for constitutional elements in ultralight metallic materials. Their advantages can be listed as follows:

1. The closed monolayer structure provides relatively low effective density of single large-sized buckyball;
2. High values of mechanical parameters. These high values make fullerenes very strong and rigid.
3. Carbon and graphite are "familiar" with many metals and alloys largely used in industry.

There is a great experience in their applications which is very useful in elaboration of new processing regimes and materials having carbon derivates in their composition.

Although the properties of the carbon atomic crystals are in focus of a large number of current publications, there is a lack of information on their mechanical characteristics, especially for fullerenes. More data are available for graphene and nanotubes. The main mechanical parameters for some carbon atomic crystals, metals and alloys are given in Table 6.

Table 6. Comparison of mechanical properties for some materials [12–16]

Tabela 6. Porównanie właściwości mechanicznych wybranych materiałów [12–16]

Material	**Young's modulus, GPa**	**Tensile strength, GPa**	**Density for a solid, kg·m^{-3}**
Carbon nanotube	–	Theoretical prediction up to 300	37–1300 [17]*
Carbon nanotube SWNT [17–20]	from 1000 to 5000	13–100^{E}	550 (37 for SWNT forest) [15]
Carbon nanotube Armchair SWNT [21]	940^{T}	126.2^{T}	
Carbon nanotube Zigzag SWNT [21]	940^{T}	94.5^{T}	
Carbon nanotube Chiral SWNT [21]	920		
Carbon nanotube MWNT [22, 23]	270^{E}–950^{E}	11^{E} – 67^{E}	–
Carbon nanofoam [24]	–	–	2–10 [25, 26]
Colossal carbon tube [20]	–	6.9^{E}	11^{T} (116^{T} of tube walls)
Carbon nanotube composites [27]	–	1.2	–
Graphene	–	130 [28]	> 1000 [29]
Diamond (C)	1220	2.8	3500
Stainless steel	0.186^{E} [30]–0.214^{E} [31]	0.38^{E} [30]–1.55^{E} [31]	7700–8100
Kevlar [32]	0.06^{E}–0.18^{E}	3.6^{E}–3.8^{E}	~2
Brass and bronze	100–125	0.55	5300
Titanium alloy (6% Al, 4% V)	105–120	0.9	4510
Copper (Cu)	117	0.22	8920
Silicon [33]	185	–	2329
Beryllium (Be)	287	0.448	1840
Molybdenum (Mo)	329	0.734	10280
Tungsten (W)	400–410	1.51	19250
Sapphire (Al_2O_3)	435	1.9	3900–4100
Silicon carbide (SiC)	450	3.44	3210 [34]
Osmium (Os)	550	–	22 580
Tungsten carbide (WC)	450–650	–	15 800

Notes: ^{E} – Experimental observation; ^{T} – Theoretical prediction, SWNT – single-walled carbon nanotube, DWNT – double-walled carbon nanotubes, MWNT – multi-walled carbon nanotubes.
** strongly depends on production method.*

It can be seen from this table that in fact all types of carbon atomic crystals, carbon nanofoams and colossal carbon tubes have the values of Young's modulus and tensile strength many times higher than all widely used metallic and nonmetallic materials. In terms of the tensile strength, graphene is the stiffest and strongest material ever discovered. This fact is explained by the nature of chemical bonding between the individual carbon atoms entirely composed of sp^2 bonds. On this basis it can be considered as a promising reinforcing phase in various metal matrix composites. In the case of fullerenes, sp^2 bonds are also responsible for an unusually high value of the mechanical characteristics. Special attention deserves MWNT which seems to be the strongest version of nanotubes and maybe of fullerens, too.

Fullerenes (Carbon tubes and buckyballs)

Below we will estimate the relation between the number of carbon atoms which build a certain fullerene and its effective density. Here the term "effective density" means the ratio between the weight of the total number of atoms in the fullerene structure considered and the volume of the fullerene. In the case of buckyballs and tubes, the volume, *V*, is calculated, respectively, from relations

$$V = \frac{4}{3}\pi\left(\frac{d}{2}\right)^3 \tag{10}$$

$$V = \pi\left(\frac{d}{2}\right)^2 H \tag{11}$$

Where *d* is the diameter of the fullerene and *H* is the length of the tube. The weight of one carbon atom, G_C, is the ratio between standard atomic weight (12.0107 g·mole^{-1} for carbon) and Avogadro constant (6.0221 x 10^{23} mole^{-1}), i.e. G_C = 1.9944 x 10^{-26} kg.

Buckyballs are spherical closed construction (polyhedron) of hexagons and pentagons in the vertices of which are displaced carbon atoms, see Fig. 5 a) and b). In geometrical terms, the number of vertices, N_C, the number of faces, *F*, and the number of edges, *E*, obey the relation [11]

$$N_C - E + F = 2 \tag{12}$$

The number of pentagons is exactly 12 for all buckyballs and the number of hexagons is $N_c/2 - 10$. The bond length in graphene is a = 0.142 nm. Here it is assumed that the hexagons are regular and all sides are of same length a. The area of such hexagon is

$$S_6 = 6\frac{a^2}{4tg30^\circ} \tag{13}$$

By analogy the area of a regular pentagon is

$$S_5 = 6\frac{a^2}{4tg36^\circ} \tag{14}$$

The total area, Σ_N of certain buckyball can be estimated by the sum:

$$\Sigma_N = 12S_5 + (N_C/2 - 10)S_6 \tag{15}$$

The diameter of this buckyball is obtained from the relation

$$d = \sqrt{\frac{\Sigma_N}{\pi}} \tag{16}$$

and its volume calculated by formula (10), where d is the diameter taken from (16). The mass of the buckyball, M_N, with N_C atoms in its construction is

$$M_N = N_C G_C \tag{17}$$

and the effective density of the buckyball is determined by relation

$$\rho_{eff} = \frac{M_N}{V} = \frac{6\sqrt{\pi}M_N}{(12S_5 + (N_C/2 - 10)S_6)^{3/2}} \tag{18}$$

In this way for each buckyball of N_C carbon atoms we can calculate its diameter by (16) and its effective density by (18). The results are shown in Fig. 6.

According to available information the largest carbon molecule registered up to now is C_{560} but our calculations are carried out for a number of atoms very far from 560. For C_{560} molecule the effective density is 2137 kg·m^{-3}, Fig. 6 a), and the diameter is 2.15 nm, Fig. 6 b). The effective density becomes lower than 1.2 kg·m^{-3} (air density at sea level) for number of atoms in the buckyball molecule greater than 17.3 x 10^8, Fig. 6 c) and diameter larger than of 3.8 μm, Fig. 6 d).

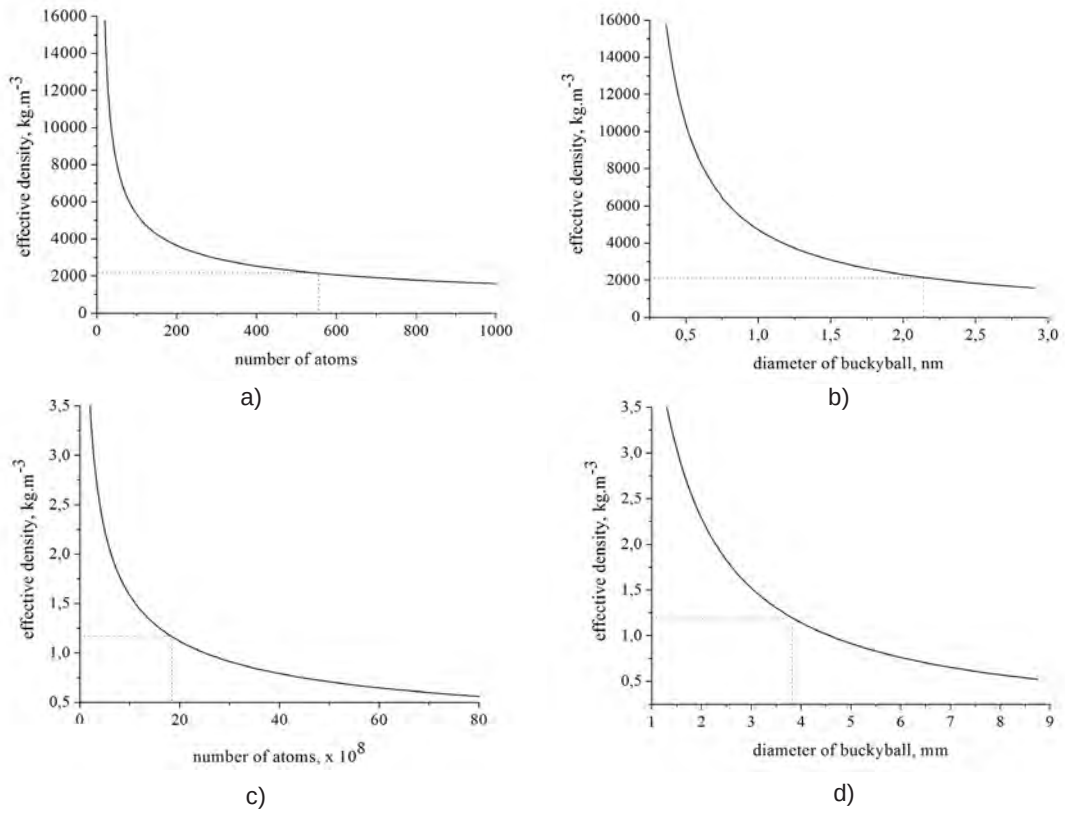

Fig. 6. Calculated effective density of buckyballs as function of: a), c) number of carbon atoms in molecule; b), d) diameter of buckyball; a), b) for small number of carbon atoms and c), d) for large number of carbon atoms

Rys. 6. Obliczona efektywna gęstość „piłeczek Bucky'ego" w funkcji: a), c) liczby atomów węgla w cząsteczce; b), d) średnicy „piłeczek Bucky'ego"; a), b) dla małej liczby atomów węgla; c), d) dla dużej liczby atomów węgla

To be used as ingredients for ultralight synthetic foams as shown in Fig. 1, a carbon buckyball of diameter d_0 must be coated with some materials which must play the role of glue. Let us denote the diameter of the coated ball by d. Then the mass of the "nude" buckyball is

$$M_N = \frac{4\pi}{3}\left(\frac{d_0}{2}\right)^3 \rho_{eff} \tag{19}$$

and the mass, M_C, of the coating is

$$M_C = \frac{4\pi}{3}\left[\left(\frac{d}{2}\right)^3 - \left(\frac{d_0}{2}\right)^3\right]\rho_c \tag{20}$$

where ρ_C is the density of the coating substance. The total density, ρ_{tot}, of the coated buckyball can be expressed by the relation

$$\rho_{tot} = \frac{M_N + M_C}{\frac{4}{3}\pi\left(\frac{d}{2}\right)^3} \tag{21}$$

In the case considered here the values of ρ_{eff} are small, see Fig. 6 d), and the density of coating substance, usually metal, is very high with respect to ρ_{eff}, i.e.

$$\rho_{eff} \ll \rho_C \tag{22}$$

After substitution of (19) and (20) into (21), taking into account (22), and after simple transformations, we obtain

$$\rho_{tot} = \rho_C\left[1 - \left(\frac{d_0}{d}\right)^3\right] \tag{23}$$

For coated buckyball with total density smaller than certain value R, the following must be valid

$$\rho_C \left[1 - \left(\frac{d_0}{d}\right)^3\right] < R \tag{24}$$

After solving the relation (24) in respect to d we obtain

$$d < \frac{d_0}{\sqrt[3]{1 - \frac{R}{\rho_C}}} \tag{25}$$

This expression gives information that if a buckyball is of radius d_0 and coating substance is of density ρ_C, the diameter of coated buckyball must obey relation (25) to have total density $\rho_{tot} < R$. Here we will demonstrate the use of the last relation for estimation of the coating thickness $\Delta r = 0.5(d - d_0)$. Let us consider a buckyball with diameter $d_0 = 7.61 \times 10^{-6} m$. The question is: what must be the diameter of coated buckyball if we use Ni-coating (ρ_C = 8908 kg·m^{-3}) or Al-coating (ρ_C=2700 kg·m^{-3}) to provide total density of the coated element lower than R = 1 kg·m^{-3}? We obtain d < 7.610285 x 10^{-6} m after applying (25) for Ni-coating. This means that the coating thickness must be Δr = 0.142 x 10^{-9} m. The unit cell of nickel is a face centered cube with the lattice parameter of 0.352 x 10^{-9} m which is more than the obtained coating thickness. Consequently, it is impossible to have Ni-coated buckyball with total density ρ_{tot} lower than 1 kg·m^{-3}. We obtain Δr = 0.470 x 10^{-9} m repeating the same calculations for Al. The unit cell of aluminum is a face centered cube with the lattice parameter of 0.406 x 10^{-9} m which is less than the obtained coating thickness. It can be seen comparing the two numbers that with two atomic aluminum layers on the buckyball considered it will keep the total density ρ_{tot} lower than 1 kg·m^{-3}. Here we will not discuss practical possibilities for realization of such a process.

Carbon nanotubes are another member of fullerenes family with a cylindrical nanostructure. Most remarkable feature of nanotubes is their length-to-diameter ratio of up to 132,000,000 : 1 [35], significantly larger than any other material. They can be considered as wrapping a graphene ribbon into a seamless cylinder. The diameter of such tubes is usually one or few nanometers. The nanotubes are called zigzag, Fig. 5 c), armchair, Fig. 5 d), or chiral, Fig. 5 e), depending on the way the graphene sheets are wrapped. Multi-walled nanotubes consist of two or more axially arranged single tubes. The interlayer distance is about 0.34 nm.

In the case of nanotube, the effective density can be defined as a mass-to-volume ratio of an elementary tube. We call elementary tube the smallest cylindrical configuration of carbon atoms which is repeated in the nanotube structure. It is easy to be found that for zigzag structure the number of atoms in an elementary tube is $N_C = 4n$, where n is the number of hexagons in the elementary tube. The diameter of the tube is

$$d = \frac{a}{\pi} n \tag{26}$$

where a = 0.246 nm [11]. The height, h, of the elementary zigzag tube is 3 times bond length c = 0.142 nm [36], i.e. h = 0.426 nm. The volume of the elementary tube is estimated by

$$V = \pi \frac{d^2}{4} h \tag{27}$$

For example, if a zigzag nanotube has n = 17 hexagons in its elementary tube, the diameter will be d = 1.33 nm. The number of atoms is N_C = 68, the weight of the elementary tube is $N_C\, G_C$ = 135.62 × 10^{-26} kg and its volume is 0.591 × 10^{-27} m^3. In this way we obtain the effective density for this nanotube ρ_{eff} = 2 295 kg/m^3.

Using this procedure we calculated the effective density and diameter of various nanotubes as a function of the number of atoms in their elementary tube. The results are shown in Fig. 7. For nanotube with 18 hexagons (n = 18) and the number of atoms in its elementary tube equal to 72, Fig. 7 a), the tube diameter is 1.41 nm, Fig. 7 b), and the effective density is 2165 kg·m^3. This density is almost the same as the density of graphite. If the number of the hexagons in the elementary tube is n = 32 450, the number of atoms is 129 800, and the tube has a diameter of 2.54 μm. These parameters correlate with the effective density of 1.2 kg·m^{-3}, which is the air density at sea level. All carbon tubes with diameters larger than 2.54 μm will have the effective density lower than the density of air. Of course, none of these tubes is nano but nevertheless, they are 3D atomic crystals. If such tubes can be synthesized at all, they will be promising candidates for components of MMC with density lower than air.

Another problem in application of these relatively large tubes are their open ends. When these tubes are coated, the material used will easily penetrate into the open ends and, as a result, the total density will dramaticaly increase. Because of this, it seems that the synthesis of large carbon tubes ended with appropriate buckyballs will be of crucial importance. Such constructions can be observed in nanotubes and are called carbon nanobuds [37], Fig. 5 f). In this structure, the fullerenes are covalently bonded to the outer sidewalls. Carbon nanotubes ended with buckyballs are also available.

The theoretically and experimentally obtained results show that nanotubes possess extraordinary tensile strain in axial direction and very small in radial one. To avoid the problem, it seems to be mandatory to use randomly dispersed coated tubes into ultralight material designed. It can be assumed that the following steps are to be taken in the technological process to obtain ultralight metallic materials on the basis of carbon fullerenes: 1. synthesis of large size closed carbon fullerenes (buckyballs and/or tubes); 2. coating of the fullerenes with very thin (only few atomic layers) metallic coating; 3. sticking of ordered coated buckyballs (see Fig. 3) or randomly dispersed coated tubes; 4. covering of the obtained aggregation with thin metallic layer in order to have an integrated solid body. To reduce as much as possible the density of this material it will be better to carry out all the processes listed above in vacuum.

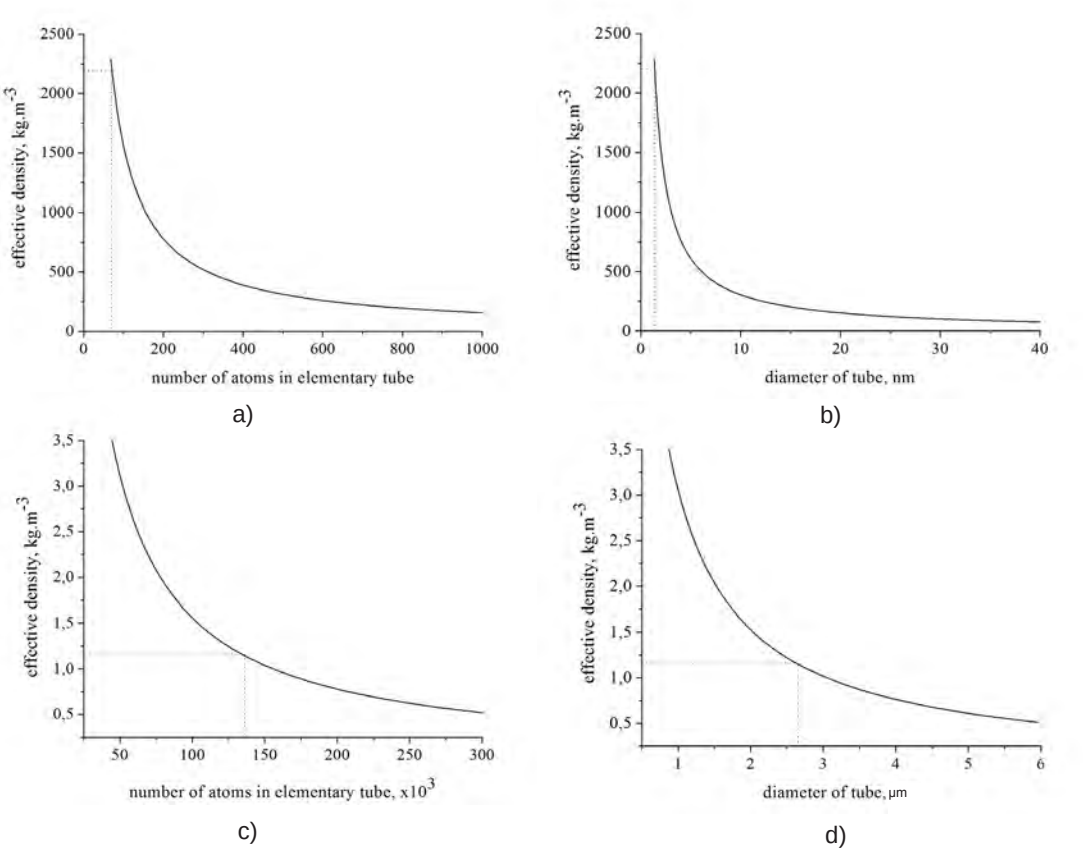

Fig. 7. Calculated effective density of nanotubes as function of: a), c) number of carbon atoms in elementary tube; b), d) diameter of carbon tube; a), b) for small number of carbon atoms and c), d) for large number of carbon atoms

Rys. 7. Obliczona efektywna gęstość nanorurek w funkcji: a), c) liczby atomów węgla w elementarnej rurce; b), d) średnicy rurki wglowej; a), b) dla małej liczby atomów węgla; c), d) dla dużej liczby atomów węgla

Special attention must be paid to onion-like buckyballs and double- or triple-walled nanotubes. Of course, their effective density is higher but they are stronger. To be used as components for ultralight composite materials and provide identical effective density, their diameter must be 1.5–2 times larger than the same diameter of conventional fullerenes. This case should be analyzed additionally.

In many industrial applications, for example in solar cells, aligned nanotubes are used. Different integrated bodies composed of aligned nanotubes can be seen in Fig. 8. They are interesting because the constructions contain large empty rooms between nanotubes. Development of special approaches to control infiltration and surface covering of aligned nanotubes can result in unexpected good results in preparation of superior light metal based materials.

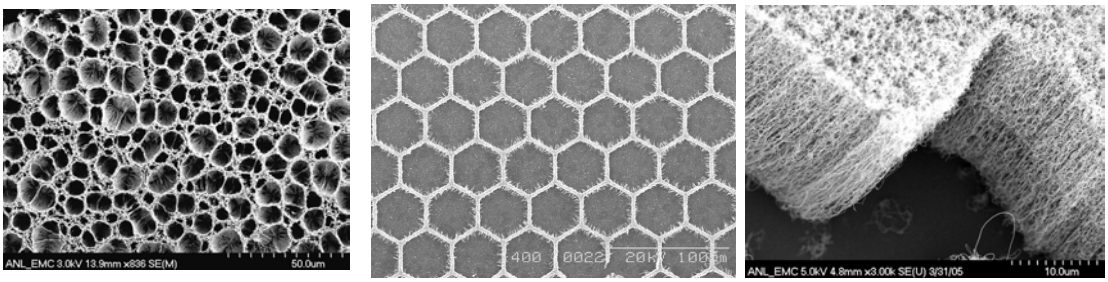

Fig. 8. Aligned nanotubes in different configurations. Images obtained in Argonne National Laboratory, USA [38]

Rys. 8. Nanorurki o różnych uporządkowanych konfiguracjach. Zdjęcia wykonane w Argonne National Laboratory, USA [38]

Other carbon materials for components of ultra light metallic composites

There are various carbon materials which are under more or less intensive investigations. Their common features are unexpected strength and low weight. Most of them have been obtained or discovered in the last 10–15 years and there are not enough data on their chemical and mechanical properties. The development of technologies for their applications is imminent. It can be expected that currently known carbon allotropic forms are not the end of such structures.

Carbon aerogels

Aerogels in general are relatively new and very interesting structures. They are obtained from a gel by replacement of the liquid component with a gas [39–41] and pretend to be the material with the lowest bulk density of any known porous solid. Important feature of the aerogels is that they have a monolithic internal structure and regular porosity. They are rigid and dry material and do not resemble a gel in their physical properties. Carbon aerogels [42] are compositions of covalently bonded nanosized particles. The pore diameter in carbon aerogels is less than 100 nm and the porosity is over 50%. The density of carbon aerogels varies in large interval and is about 200–1000 $kg \cdot m^{-3}$ [43, 44]. Integrated bodies shown in Fig. 8 are not aerogels.

Carbon nanofoam

Carbon nanofoam is another allotrope of carbon obtained in 1999 [45]. It is a 3D web constituted of strung together low-density cluster-assembly of carbon atoms. The clusters are about 6 nanometers wide and consist of about 4000 carbon atoms. Contrary to the buckyballs, in which carbon sheets are wrapped by inclusion of pentagons, in the case of nanofoam the sheets are curved by heptagons among the regular hexagonal pattern. Despite the fact that the large-scale structure of carbon nanofoam resembles that of an aerogel, the density of nanofoam is about 100 times lower than that of carbon aerogels, 2–10 $kg \cdot m^{-3}$ [24–26].

Colossal carbon tubes

Colossal carbon tubes (CCTs) are special tubular form of carbon obtained in 2008 [46, 47]. They are very different from carbon nanotubes. First, the colossal carbon tubes have much larger diameters ranging between 40 and 100 μm, Fig. 9 a) and b), and length of a few centimeters. Second, CCTs are not atomic crystals and their walls have a corrugated porous structure, similar to corrugated fiberboard, Fig. 9 c). The solid layers in the construction have a graphite-like structure. The calculated effective density of CCTs is 11 kg·m^{-3} (comparable to that of carbon nanofoams) and the density of tube walls is 116 kg·m^{-3} [20]. The axial strength of carbon nanotubes is very high but in radial direction they are extremely weak. On the other hand, in the case of CCTs the strength in both directions is almost the same.

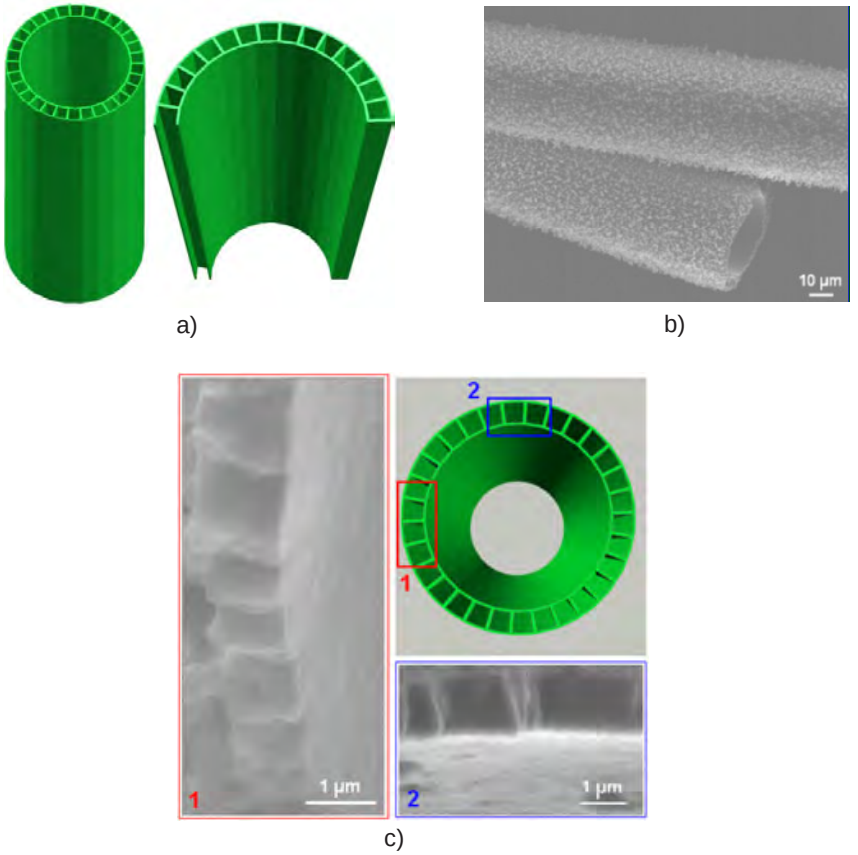

Fig. 9. Colossal carbon tubes: a) schematic illustration, after [46]; b) SEM image, side view, after [20]; c) schematic illustration and SEM images corresponding to the specific positions marked in the scheme top view of a tube, after [20]

Rys. 9. Rurki węglowe olbrzymie: a) rysunek schematyczny wg [46]; b) obraz uzyskany pod skaningowym mikroskopem elektronowym, widok boczny wg [20]; c) rysunek schematyczny i obrazy uzyskane pod skaningowym mikroskopem elektronowym odpowiadające konkretnym wybranym lokalizacjom zaznaczonym na schematycznym rysunku rurki w rzucie od góry wg [20]

Besides ultralight weight, CCTs have many attractive properties [20] such as exellent ductility and extremely high tensile strength (see also Table 3), which make them object of interest for various technical applications [48].

From the point of view of the here discussed technics for the development of ultralight metallic materials, carbon nanofoams and aerogels are similar to aligned carbon nanotubes. All of them can be covered by thin metallic layer to obtain a solid body with closed porosity. Before this process, the carbon matrix can be partially re-infiltrated with a metallic composition which will reinforce in certain degree the matrix.

Large fullerenes (single crystal tubes and buckyballs in micrometric scale) and CCTs belong to another group of components for design of ultralight materials. Before direct application they must be covered with extremely thin (few atomic layers) film which will facilitate sticking of single elements and formation of an integrated open porosity body. After this procedure the body can be covered again with more or less thin layer to form an ultralight metallic material. It seems that CCTs are most suitable for this purpose because of their size, unusual mechanical properties and known technology for production. Let us mention that large fullerenes have not yet been obtained.

Non-carbon objects for construction of ultralight materials

Fullerenes and especially nanotubes synthesized from various inorganic non-carbon materials are object of interest in many scientific publications but they have so far attracted surprisingly little attention. Initially such structures were observed in naturally formed minerals [49, 50]. First inorganic artificial nanotubes were obtained in 1992 [51] from tungsten disulfide. At present, two and three dimensional analogues of carbon atomic crystals are synthesized from: copper and bismuth [52], boron nitride, silicon, titanium dioxide, molybdenum disulfide, dichalcogenides and others [53]. They are not as light and strong as carbon derivatives but it is possible to find among them objects suitable for design of ultralight materials.

There are other non-carbon based materials with great potential to be used as components in ultralight metallic materials. Most popular of them is silica aerogel [54] which is the most extensively studied and used aerogel. Silica aerogel holds 15 entries in Guinness World Records [44] for material properties, including best insulator and lowest-density solid.

Alumina aerogel [55] is made from Al_2O_3 and has a density of 40 $kg \cdot m^{-3}$ [56]. This material is also of high potential for component of ultralight materials. Nickel coating of this aerogel will facilitate application of aluminum alloys as a cover layer.

Conclusions

The brief analysis discussed above gives us reason to assert that obtaining of metallic materials lighter than air is possible to be realized in near future. The most promising materials are synthetic foams. The problems that must be overcome are mainly related with mechanical strength of the thin-wall cenospheres. Coating of these cenospheres with extremely thin metallic layers is also a serious problem. Utilization of various methods for metal vapor atomization may be one of the fruitful ways in obtaining of such thin coatings. Other problems related with cenospheres compacting (arrangement, sticking and final coating) can be solved easier again on the basis of vapor atomization technique.

Some types of aerogels also deserve special attention, and silica and alumina aerogels are most favorable of them. For partial infiltration of such construction, pressure infiltration equipment, both gas and squeeze, can be successfully used.

References:

1. Drenchev L., Sobczak J.J., Malinov S., Sha W.: Gasars: a class of metallic materials with ordered porosity, Materials Science and Technology, 2006, Vol. 22, No. 10, pp. 1135–47 (13).
2. Lightweight Structural Members, United States Patent 7,582,361, September 1, 2009. Authors: Purgert, Robert M. (Brooklyn Heights, OH); Sobczak, Jerzy J. (Krakow, PL); Boyd, Jr. Lawrence C. (Shaker Heights, OH); Singh, Nipendra P. (Pepper Pike, OH); Bardes, Bruce P. (Montgomery, OH).
3. Groom D.E.: Abridged from Atomic Nuclear Properties. Particle Data Group: 2007, http://pdg.lbl.gov/2007/reviews/atomicrpp.pdf.
4. Drenchev L., Sobczak J.J., Malinov S., Sha W.: Modelling of structural formation in ordered porosity metal materials, Modelling Simul. Mater. Sci. Eng., 2006, Vol. 14, No. 4, pp. 663–675, doi:10.1088/0965-0393/14/4/009.
5. Xie Z., Ikeda T., Okuda Y., Nakajima H.: Sound absorption characteristics of lotus-type porous copper fabricated by unidirectional solidification, Materials Science and Engineering: 2004, A, Vol. 386, No. 1-2, pp. 390–395, doi:10.1016/j.msea.2004.07.058
6. http://en.wikipedia.org/wiki/Metal_foam.
7. Sobczak J.J., Sobczak N., Asthana R., Wojciechowski A., Pietrzak K., Rudnik D.: Atlas of Cast Metal-Matrix Composite Structures, Part I, Qualitative analysis, Motor Transport Institute – Warsaw, Foundry Research Institute – Krakow, 2007.
8. Fullerene, Encyclopedia Britannica *on-line.*
9. Iijima S.: Direct observation of the tetrahedral bonding in graphitized carbon black by high resolution electron microscopy, Journal of Crystal Growth, 1980, Vol. 50, No. 3, pp. 675–683, doi:10.1016/0022-0248(80)90013-5.
10. http://en.wikipedia.org/wiki/Fullerene.
11. http://en.wikipedia.org/wiki/Carbon_nanotubes.
12. Bellucci S.: Carbon nanotubes: physics and applications, Physica Status Solidi, 2005, (c), Vol. 2, No. 1, pp. 34–47, doi:10.1002/pssc.200460105.
13. Chae H. G., Satish K.: Rigid-rod Polymeric Fibers, Journal of Applied Polymer Science, 2006, Vol. 100, No. 1, pp. 791–802, doi:10.1002/app.22680.
14. Meo M., Rossi M.: Prediction of Young's modulus of single wall carbon nanotubes by molecular-mechanics-based finite element modelling, Composites Science and Technology, 2006, Vol. 66, Nos. 11–12, pp. 1597–1605, doi:10.1016/j.compscitech.2005.11.015.
15. Sinnott S.B., Rodney A., Andrews R.: Carbon Nanotubes: Synthesis, Properties, and Applications, Critical Reviews in Solid State and Materials Sciences, 2001, Vol. 26, No. 3, pp. 145–249, doi:10.1080/20014091104189.
16. http://en.wikipedia.org/wiki/Tensile_strength.
17. Collins P.G.: Nanotubes for Electronics, Scientific American Magazine, 2000, pp. 67–69, http://www.crhc.uiuc.edu/ece497nc/fall01/papers/NTs_SciAm_2000.pdf.
18. Jensen K., Mickelson W., Kis A., Zettl A.: Buckling and kinking force measurements on individual multiwalled carbon nanotubes, Phys. Rev., 2007, B, Vol. 76, p.195436.
19. Lee C. et al. „Measurement of the Elastic Properties and Intrinsic Strength of Monolayer Graphene". Science 2008, 321 (5887), p.385-397.
20. Peng H., Chen D., Huang J.Y. et al.: Strong and Ductile Colossal Carbon Tubes with Walls of Rectangular Macropores, Phys. Rev. Lett, 2008, Vol. 101, No.14, pp. 145501, doi:10.1103/PhysRevLett.101.145501
21. http://en.wikipedia.org/wiki/Carbon_nanotube.

22. Min-Feng Yu, Lourie O.M., Dyer J., Moloni K., Kelly T.F., Ruoff R.S.: Strength and Breaking Mechanism of Multiwalled Carbon Nanotubes Under Tensile Load, Science, 2000, Vol. 287, No. 5453, pp. 637–640. doi:10.1126/science.287.5453.637.
23. Demczyk B.G., Wang Y.M., Cumings J., Hetman M., Han W., Zettl A., Ritchie R.O.: Direct mechanical measurement of the tensile strength and elastic modulus of multiwalled carbon nanotubes", Materials Science and Engineering, 2002, A, Vol. 334, Nos. 1–2, pp. 173–178, doi:10.1016/S0921-5093(01)01807-X.
24. Rode A.V., et al.: Structural analysis of a carbon foam formed by high pulse-rate laser ablation, Applied Physics A: Materials Science & Processing, 1999, Vol. 69, No. 7, pp. S755–S758, doi:10.1007/s003390051522.
25. http://en.wikipedia.org/wiki/Carbon_nanofoam
26. Rode A.V. et al.: Unconventional magnetism in all-carbon nanofoam, Phys. Rev., 2004, B, Vol. 70, No. 5, pp. 054407.
27. Wang Z., Ciselli P., Peijs T.: The extraordinary reinforcing efficiency of single-walled carbon nanotubes in oriented poly (vinyl alcohol) tapes, Nanotechnology, 2007, Vol. 18, No. 45, pp. 455709, IOP.org.
28. Lee C. et al.: Measurement of the Elastic Properties and Intrinsic Strength of Monolayer Graphene, Science, 2008, Vol. 321, No. 5887, pp.385-388, doi:10.1126/science.1157996. http://www.sciencemag.org/cgi/content/abstract/321/5887/385.
29. http://en.wikipedia.org/wiki/Graphene.
30. Australian Stainless Steel Development Association (ASSDA) - Properties of Stainless Steel.
31. Stainless Steel - 17-7PH (Fe/Cr17/Ni 7) Material Information.
32. Wagner H.D.: Reinforcement, Encyclopedia of Polymer Science and Technology, John Wiley &Sons, 2002, doi:10.1002/0471440264.pst317, http://www.weizmann.ac.il/wagner/COURSES/Reading%20material%20(papers)/Encyclopedy_of_polymer_science_2003.pdf.
33. http://www.ioffe.ru/SVA/NSM/Semicond/Si.
34. Patnaik P.: Handbook of Inorganic Chemicals. McGraw-Hill, 2002.
35. Wang X., Li Q., Xie J., Jin Z., Wang J., Li Y., Jiang K., Fan S.: Fabrication of Ultralong and Electrically Uniform Single-Walled Carbon Nanotubes on Clean Substrates, Nano Letters 9, Vol. 9, 2009, pp. 3137–3141, doi:10.1021/nl901260b.
36. Hembacher S., Giessibl F. J., Mannhart J., Quate C. F.: Revealing the hidden atom in graphite by low-temperature atomic force microscopy, Procceedings of The National Academy of Sciences of the USA, 2003, Vol. 100, No. 22, pp. 12539–12542, doi: 10.1073/pnas.2134173100, www.pnas.org/cgi/doi/10.1073/pnas.2134173100.
37. http://en.wikipedia.org/wiki/Carbon_nanobud.
38. http://www.flickr.com/photos/argonne/3974996522.
39. Taher A.: Scientists hail 'frozen smoke' as material that will change world, News Article, London: Times Online, 2007-08-19, Retrieved 2007-08-22.
40. Kistler S.S.: Coherent expanded aerogels and jellies, Nature, 1931, Vol. 127, No. 3211, pp. 741, doi:10.1038/127741a0.
41. Kistler S.S.: Coherent Expanded-Aerogels, Journal of Physical Chemistry, 1932, Vol. 36, No. 1, pp. 52–64, doi:10.1021/j150331a003.
42. Pekala R.W.: Organic aerogels from the polycondensation of resorcinol with formaldehyde, Journal of Material Science, 1989, Vol. 24, No. 9, pp. 3221–3227, doi:10.1007/BF01139044.
43. http://en.wikipedia.org/wiki/Carbon_nanofoam
44. Guinness Records Names JPL's Aerogel World's Lightest Solid, News Article. Jet Propulsion Laboratory, 2002-05-07, http://stardust.jpl.nasa.gov/news/news93.html. Retrieved 2009-05-25.
45. Rode, Andrei V.; et al. (1999). „Structural analysis of a carbon foam formed by high pulse-rate laser ablation". Applied Physics A: Materials Science & Processing 69 (7): S755–S758.
46. Carbon nanotubes, but without the 'nano', Aug. 2008, http://physicsworld.com/cws/article/news/35364. Retrieved 2009-08-03.

47. Peng, H.; Chen, D.; et al., Huang J.Y. et al.: „Strong and Ductile Colossal Carbon Tubes with Walls of Rectangular Macropores". Phys. Rev. Lett., 2008, 101 (14): 145501. The Space Elevator Feasibility Condition, http://www.spaceward.org/elevator-feasibility.
48. The Space Elevator Feasibility Condition, http://www.spaceward.org/elevator-feasibility.
49. Tenne R., Margulis L., Genut M., Hodes G.: Polyhedral and cylindrical structures of tungsten disulphide, Nature, 1992, Vol. 360, No. 6403, pp. 444–446, doi:10.1038/360444a0.
50. Pauling L.: The Structure Of The Chlorites, Proc. Natl. Acad. Sci. U.S.A., 1930, Vol. 16, No. 9, pp. 578–82. doi:10.1073/pnas.16.9.578. PMC 526695. PMID 16587609.
51. Harris, P.F.J.: Carbon nanotubes and related structures (1st ed.). Cambridge University Press, 2002, pp. 213–32.
52. Dachi Yang, Guowen Meng, Shuyuan Zhang, Yufeng Hao, Xiaohong An, Qing Wei, Min Ye, Lide Zhang: Electrochemical synthesis of metal and semimetal nanotube–nanowire heterojunctions and their electronic transport properties, Chem. Commun., 2007, pp. 1733–1735, doi:10.1039/B614147A, http://pubs.rsc.org/en/Content/ArticleLanding/2007/CC/b614147a.
53. Novoselov K.S. et al.: Two-dimensional atomic crystals, Procedings of the National Academy of Sciences of the U.S.A., 2005, Vol. 102, No. 30, pp. 10451–10453, doi:10.1073/pnas.0502848102, http://onnes.ph.man.ac.uk/nano/Publications/PNAS_2005.pdf.
54. http://www.aerogel.org/?p=16.
55. Poco J.F., Satcher Jr J H., Hrubesh L. W.: Synthesis of high porosity, monolithic alumina aerogels, Journal of Non-Crystalline Solids, 2001, Vol. 285, No. 1–3, pp. 57–63, doi: 10.1016/S0022-3093(01)00432-X.
56. http://www.aerogel.org/?p=1022.